

Electronic Supplementary Information (ESI) For

## Three Zn(II) Coordination Polymers Constructed with a New Amide-thiophene-derived Bis-pyridyl Ligand as Ultrasensitive Luminescent Sensors for Hg(II) and Purines

Xiuli Wang<sup>\*a</sup>, Jianxin Ma<sup>a,b</sup>, Na Xu<sup>a</sup>, Yue Wang<sup>a</sup>, Jiayu Sun<sup>a</sup>, and Guocheng Liu<sup>a</sup>

<sup>a</sup> College of Chemistry and Materials Engineering, Bohai University, Professional Technology Innovation Center of Liaoning Province for Conversion Materials of Solar Cell, Jinzhou 121013, P. R. China

<sup>b</sup> School of Materials science and Engineering, Changchun University of Science and Technology, Changchun 130022, P. R. China

### S1. X-ray Crystallography

The single-crystal diffraction data for LCPs **1-3** were collected by using a Bruker SMART APEXII CCD diffractometer at 293 K with Mo  $K\alpha$  radiation ( $\lambda = 0.71073 \text{ \AA}$ ). The structures were solved by direct methods and refined by full matrix least-squares on  $F^2$  employing the OLEX2 program.<sup>1</sup> All crystal data and detailed structural refinement results are summarized in Table S1, and selected bond lengths ( $\text{\AA}$ ) and angles ( $^\circ$ ) are listed in Table S2. The single crystal data for LCPs **1-3** have been obtained in the Cambridge Crystallographic Data Center (CCDC no: 2060451, 2089164, and 2089165).

### Materials and methods

All chemicals and reagents were purchased from commercial sources and used as received except for 4-bpft (Scheme 1). The single-crystal diffraction data for LCPs **1-3** were collected by using a Bruker SMART APEXII CCD diffractometer at 293 K with Mo  $K\alpha$  radiation ( $\lambda = 0.71073 \text{ \AA}$ ). The powder X-ray diffraction (D/teX Ultra diffractometer) and the infrared spectra (Varian 640 FTIR spectrometer) were measured to confirm the structures of LCPs **1-3**. The fluorescent spectra were recorded on a Hitachi F-4500 luminescence/phosphorescence spectrometer. UV-vis absorption spectra were obtained by PerkinElmer Lambda 750. With a FLS1000 transient steady-state fluorescence spectrometer, the fluorescence lifetime could be obtained. The  $^1\text{H}$  NMR spectra was recorded on Agilent 400-MR spectrometer using DMSO- $d_6$  as a solvent.

**Table S1.** Crystallographic data for LCPs **1-3**.

LCP	LCP 1	LCP 2	LCP 3
CCDC	2060451	2089164	2089165
Empirical formula	C <sub>52</sub> H <sub>44</sub> Zn <sub>2</sub> N <sub>8</sub> O <sub>14</sub> S <sub>2</sub>	C <sub>27</sub> H <sub>22</sub> ZnN <sub>4</sub> O <sub>6</sub> S	C <sub>26</sub> H <sub>20</sub> ZnN <sub>4</sub> O <sub>7</sub> S
Formula weight	1199.81	595.91	597.89
Crystal system	Triclinic	Triclinic	Triclinic
Space group	<i>P</i> $\bar{1}$	<i>P</i> $\bar{1}$	<i>P</i> $\bar{1}$
<i>a</i> (Å)	11.9101(5)	10.0385(10)	9.8851(8)
<i>b</i> (Å)	14.8958(6)	11.1557(12)	10.8960(8)
<i>c</i> (Å)	16.5644(7)	12.4792(13)	12.2041(10)
$\alpha$ (°)	106.2430(10)	79.339(2)	82.082(2)
$\beta$ (°)	109.7700(10)	80.212(2)	80.528(2)
$\gamma$ (°)	96.0220(10)	68.539(2)	68.643(2)
<i>V</i> (Å <sup>3</sup> )	2589.55(19)	1270.1(2)	1203.18(17)
<i>Z</i>	2	2	2
<i>D</i> <sub>calc</sub> (g/cm <sup>3</sup> )	1.539	1.558	1.650
$\mu$ /mm <sup>-1</sup>	1.083	1.101	1.165
<i>F</i> (000)	1232	612	612
<i>R</i> <sub>int</sub>	0.0167	0.0229	0.0317
<i>R</i> <sub>1</sub> <sup>a</sup> [ <i>I</i> > 2 $\sigma$ ( <i>I</i> )]	0.0419	0.0409	0.0406
<i>wR</i> <sub>2</sub> <sup>b</sup> (all data)	0.1077	0.1031	0.0842
GOF	1.018	1.021	1.004
$\Delta \rho$ <sub>max</sub> (e $\cdot$ Å <sup>-3</sup> )	1.334 and -0.620	0.639 and -0.658	0.356 and -0.395

$$^a R_1 = \sum |F_o| - |F_c| / \sum |F_o|. \quad ^b wR_2 = [\sum w(F_o^2 - F_c^2)^2 / \sum w(F_o^2)^2]^{1/2}.$$

**Table S2.** Selected bond lengths (Å) and bond angles (°) for LCP **1**.

LCP 1			
Zn(2)–O(4)	2.0183(15)	Zn(1)–O(1)	1.9957(15)
Zn(2)–O(9)#1	2.1528(16)	Zn(1)–O(5)#2	2.0269(19)
Zn(2)–O(10)#1	2.2706(19)	Zn(1)–N(1)	2.163(2)
Zn(2)–O(3)	2.0793(17)	Zn(1)–O(2)	2.0329(18)
Zn(2)–N(5)	2.144(2)	Zn(1)–N(4)#2	2.166(2)
Zn(2)–N(8)#1	2.177(2)	O(2)–Zn(1)–N(4)#2	84.37(9)
O(4)–Zn(2)–O(9)#1	153.75(7)	N(5)–Zn(2)–O(9)#1	88.36(7)
O(4)–Zn(2)–O(10)#1	94.55(7)	N(5)–Zn(2)–O(10)#1	93.47(8)

O(4)–Zn(2)–O(3)	115.78(7)	N(5)–Zn(2)–N(8)#1	174.54(7)
O(4)–Zn(2)–N(5)	93.34(7)	N(8)#1–Zn(2)–O(10)#1	88.50(8)
O(4)–Zn(2)–N(8)#1	91.59(8)	O(1)–Zn(1)–O(5)#2	137.05(9)
O(9)#1–Zn(2)–O(10)#1	59.20(6)	O(1)–Zn(1)–N(1)	93.90(7)
O(9)#1–Zn(2)–N(8)#1	88.27(7)	O(1)–Zn(1)–O(2)	121.98(8)
O(3)–Zn(2)–O(9)#1	90.41(7)	O(1)–Zn(1)–N(4)#2	93.73(8)
O(3)–Zn(2)–O(10)#1	149.33(6)	O(5)#2–Zn(1)–N(1)	88.82(8)
O(3)–Zn(2)–N(5)	89.43(8)	O(5)#2–Zn(1)–O(2)	100.97(9)
O(3)–Zn(2)–N(8)#1	86.30(8)	O(5)#2–Zn(1)–N(4)#2	90.46(8)
O(2)–Zn(1)–N(1)	85.52(9)	N(1)–Zn(1)–N(4)#2	169.54(8)

Symmetry codes: #1 -x,-y+2,-z+1, #2 -x+1,-y+1,-z+1

**Table S3.** Selected bond lengths (Å) and bond angles (°) for LCP 2.

LCP 2			
Zn(1)–O(1)	2.0032(18)	Zn(1)–N(1)#3	2.191(3)
Zn(1)–O(2)#1	2.060(2)	Zn(1)–O(5)#2	2.348(2)
Zn(1)–O(3)#2	2.19(2)	Zn(1)–N(2)	2.177(3)
N(2)–Zn(1)–N(1)#3	171.39(8)	O(2)#1–Zn(1)–O(3)#2	91.2(6)
O(1)–Zn(1)–O(2)#1	117.72(8)	O(2)#1–Zn(1)–N(1)#3	83.52(9)
O(1)–Zn(1)–O(3)#2	150.3(7)	O(2)#1–Zn(1)–O(5)#2	150.35(8)
O(1)–Zn(1)–N(1)#3	91.41(8)	O(2)#1–Zn(1)–N(2)	88.74(9)
O(1)–Zn(1)–O(5)#2	90.34(8)	O(3)#2–Zn(1)–O(5)#2	60.0(7)
O(1)–Zn(1)–N(2)	95.53(9)	N(1)#3–Zn(1)–O(3)#2	84.9(5)
O(1)–Zn(1)–O(10)#2	146.3(7)	N(1)#3–Zn(1)–O(5)#2	86.61(9)
N(2)–Zn(1)–O(5)#2	98.41(9)	N(2)–Zn(1)–O(3)#2	91.6(5)
O(10)#2–Zn(1)–N(2)	84.9(6)		

Symmetry codes: #1 -x+1, -y, -z+1, #2 x-1, y, z, #3 -x, -y, -z+1

**Table S4.** Selected bond lengths (Å) and bond angles (°) for LCP 3.

LCP 3			
Zn(1)–O(1)#1	1.983(2)	Zn(1)–N(1)#2	2.196(3)
Zn(1)–O(2)	1.979(2)	Zn(1)–N(2)	2.179(3)
Zn(1)–O(3)#2	2.034(2)	O(2)–Zn(1)–N(1)#2	88.56(9)
O(1)#1–Zn(1)–O(3)#2	129.41(9)	O(2)–Zn(1)–N(2)	91.57(10)

O(1)#1–Zn(1)–N(1)#2	95.12(10)	O(3)#2–Zn(1)–N(1)#2	87.67(9)
O(1)#1–Zn(1)–N(2)	90.78(10)	O(3)#2–Zn(1)–N(2)	84.86(9)
O(2)–Zn(1)–O(1)#1	128.32(9)	N(2)–Zn(1)–N(1)#2	172.37(10)
O(2)–Zn(1)–O(3)#2	102.21(9)		

Symmetry codes: #1 x+1, y, z, #2 -x+1, -y+2, -z

**Table S5.** Comparison of fluorescent property of LCPs 1–3 for sensing Hg(II).

Fluorescent sensing materials	$K_{sv}$ ( $M^{-1}$ )	Detection Limit (M)	Medium	Ref.
LCP 1	$5.44 \times 10^4$	$9.83 \times 10^{-7}$	H <sub>2</sub> O	This work
LCP 2	$6.07 \times 10^3$	$8.84 \times 10^{-6}$	H <sub>2</sub> O	This work
LCP 3	$2.43 \times 10^3$	$2.21 \times 10^{-5}$	H <sub>2</sub> O	This work
CdTe QD	–	$1.0 \times 10^{-8}$	H <sub>2</sub> O/MeCN	2
Au/N–CQDs	–	$1.18 \times 10^{-7}$	H <sub>2</sub> O	3

**Table S6.** Comparison of fluorescent property of LCP 1 for sensing adenine.

Fluorescent sensing materials	$K_{sv}$ ( $M^{-1}$ )	Detection Limit (M)	Medium	Ref.
LCP 1	$1.103 \times 10^4$	$4.83 \times 10^{-6}$	H <sub>2</sub> O	This work
L–Tryptophan–Cu <sup>2+</sup>	–	$0.046 \times 10^{-6}$	H <sub>2</sub> O	4
GO–PANI	–	$1.3 \times 10^{-5}$	H <sub>2</sub> O	5
N–GN	–	$8.0 \times 10^{-5}$	DMA	6

**Table S7.** Comparison of fluorescent property of LCP 1 for sensing guanine.

Fluorescent sensing materials	$K_{sv}$ ( $M^{-1}$ )	Detection Limit (M)	Medium	Ref.
LCP 1	$8.99 \times 10^4$	$5.97 \times 10^{-6}$	H <sub>2</sub> O	This work
CDs	–	$0.67 \times 10^{-7}$	H <sub>2</sub> O	7
CdTe nanoparticles	–	$8 \times 10^{-8}$	H <sub>2</sub> O	8
Cu <sup>2+</sup> -nuclear	–	$1.9 \times 10^{-6}$	H <sub>2</sub> O	9
GO–PANI	–	$1.36 \times 10^{-5}$	H <sub>2</sub> O	10

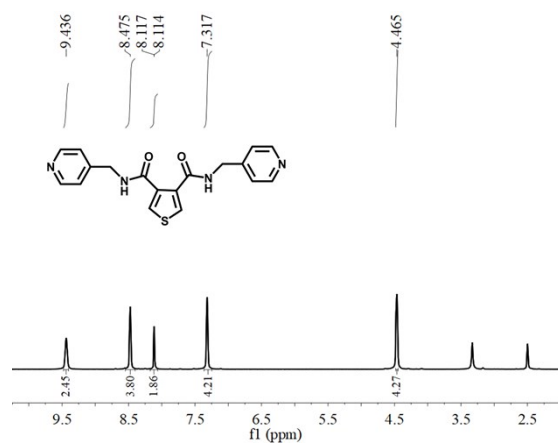


**Fig. S1.**  $^1\text{H}$  NMR spectrum of 4-bpft in  $\text{DMSO-}d_6$ .

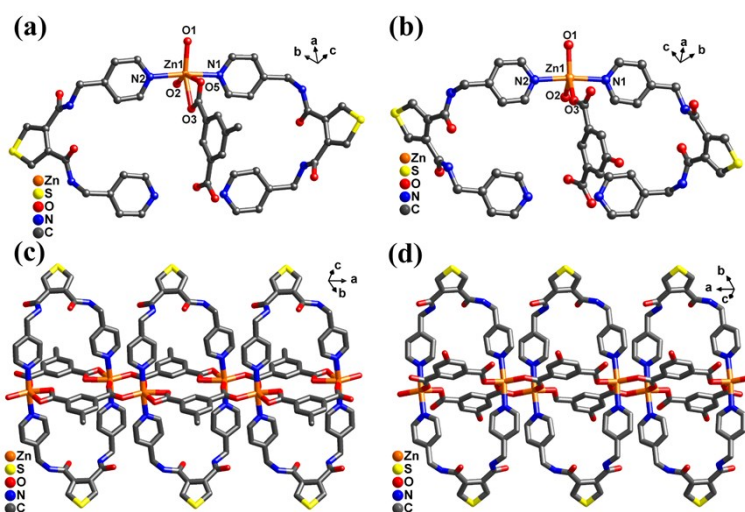


**Fig. S2.** The coordination environment of  $\text{Zn(II)}$  in LCP 2 (a) and LCP 3 (b). The 1D structure of LCP 2 (c) and LCP 3 (d).

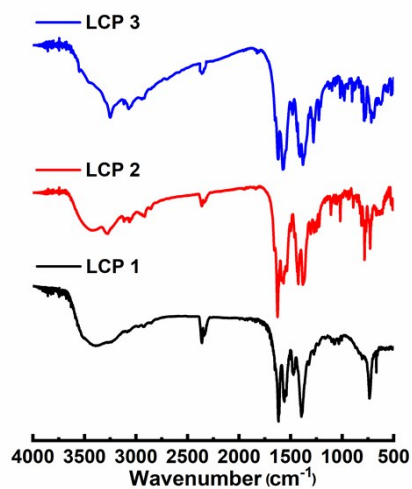


**Fig. S3.** The IR spectra of LCPs 1–3.

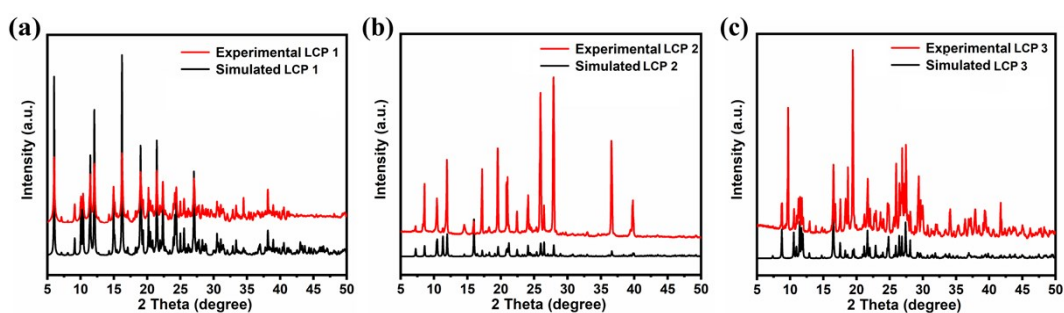


**Fig. S4.** The PXRD patterns of LCPs 1–3.

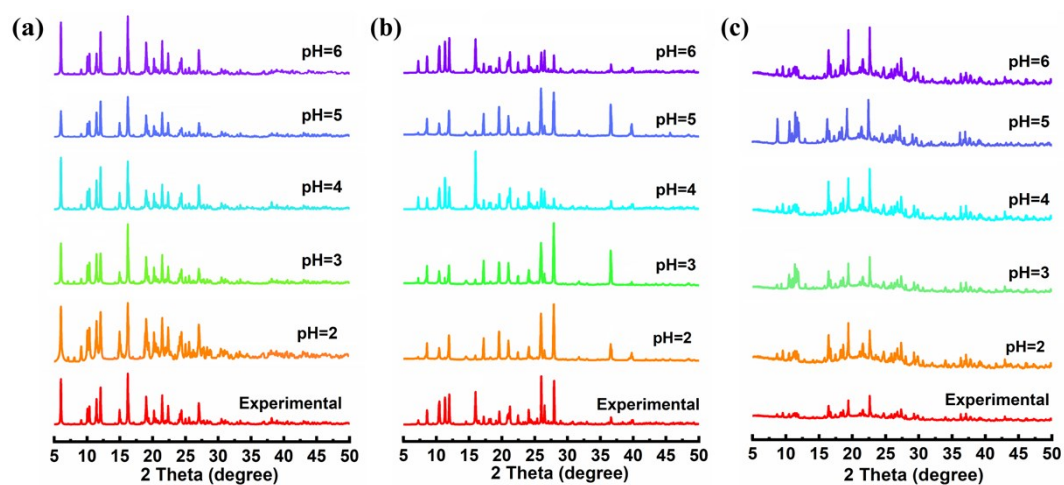


**Fig. S5.** The PXRD patterns of LCPs 1–3 before and after being soaked in acidic and basic solutions for 12 h with a wide pH range of 2.0 ~ 6.0.

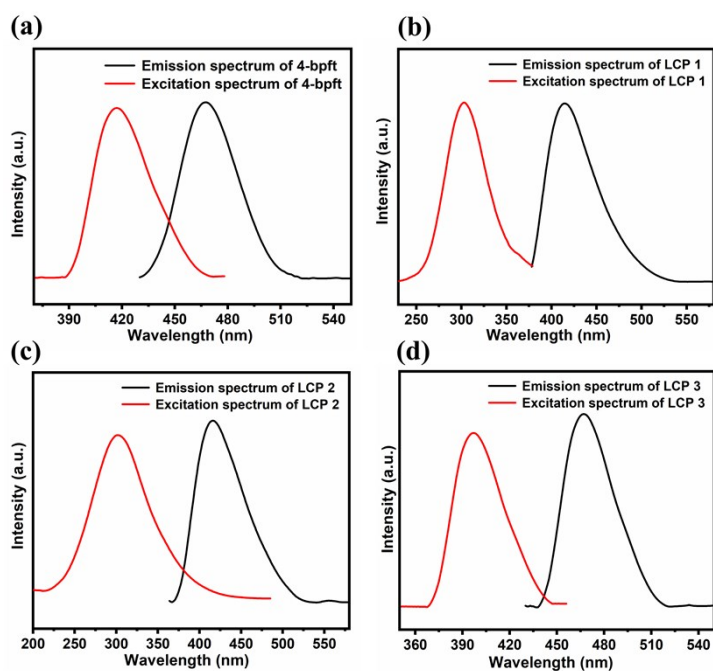


**Fig. S6.** The solid excitation and emission spectra of 4-bpft and LCPs 1–3.

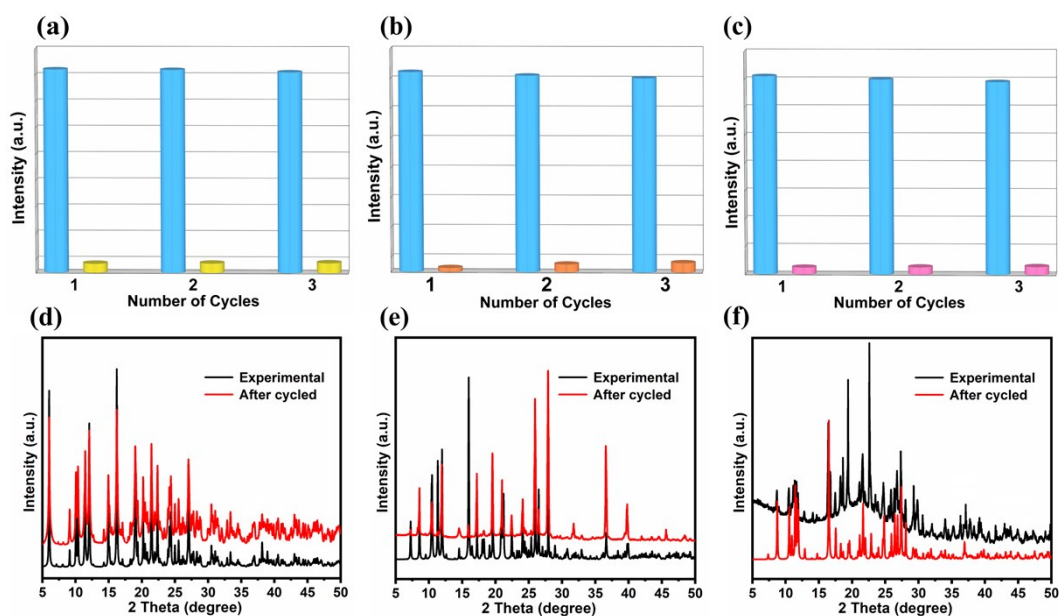


**Fig. S7.** The cyclic response of the luminescence intensities for detecting Hg(II) of LCP 1 (a), LCP 2 (b), and LCP 3 (c); The PXRD patterns treated by Hg(II) of LCP 1 (d), LCP 2 (e), and LCP 3 (f).

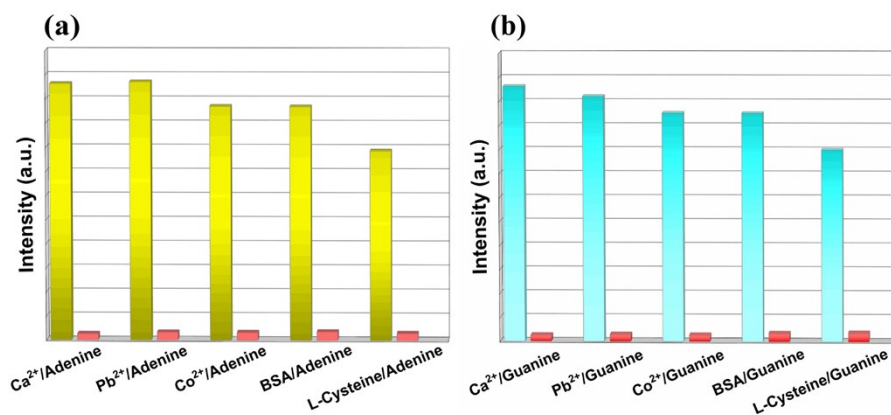


**Fig. S8.** Competitive quenching experiments of LCP 1 for the selective recognition of adenine (a) and guanine (b).

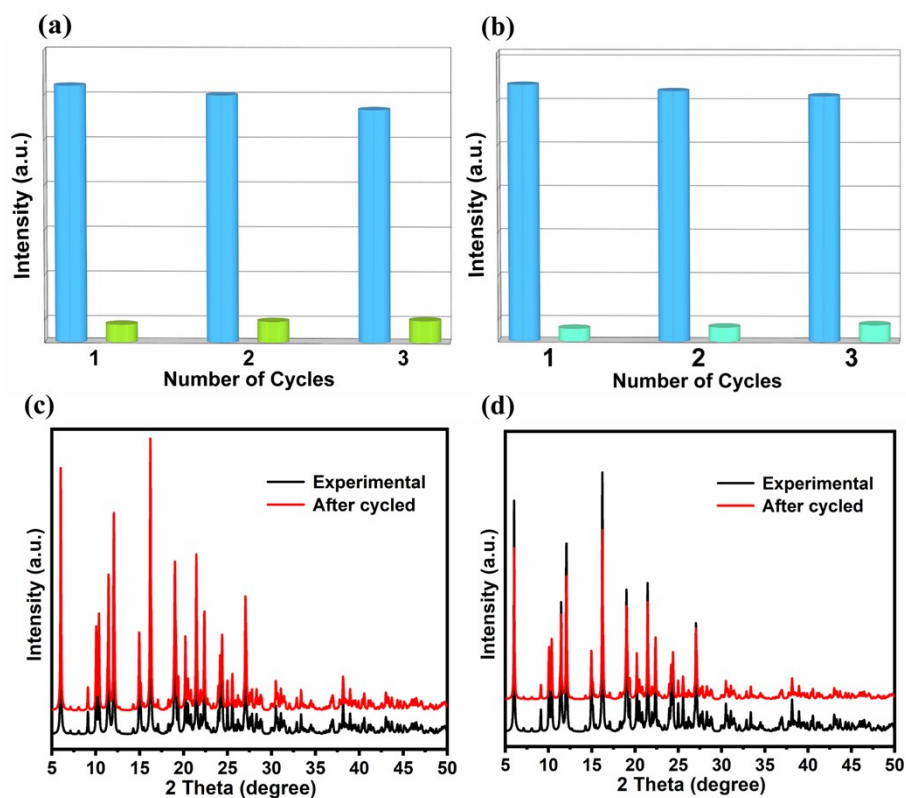


**Fig. S9.** The cyclic response of the luminescence intensities of LCP 1 for detecting of adenine (a) and guanine (b); The PXRD patterns of LCP 1 treated by adenine (c) and guanine (d).

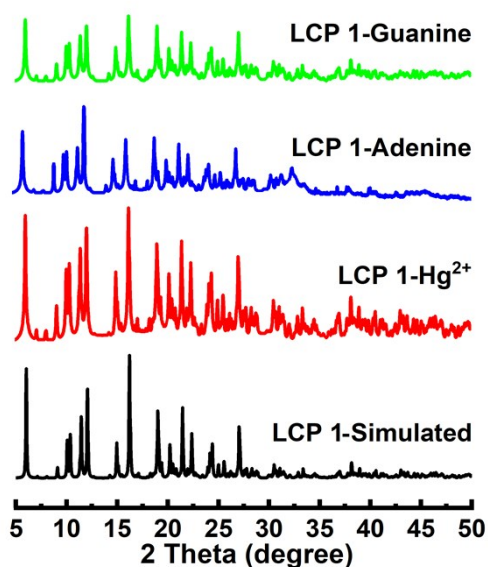


**Fig. S10.** The PXRD of LCP 1 after soaked in different analytes solution for 24h.

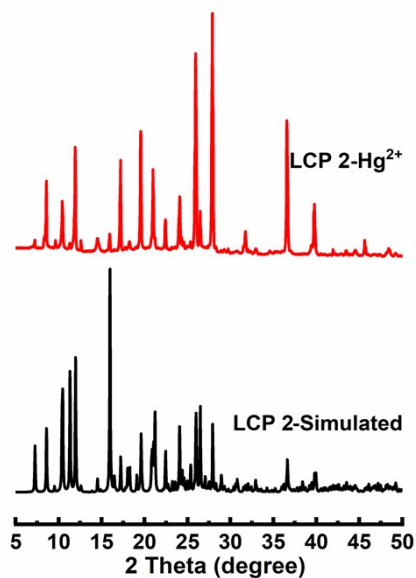


**Fig. S11.** The PXRD of LCP 2 after immersing in Hg(II) solution for 24h.

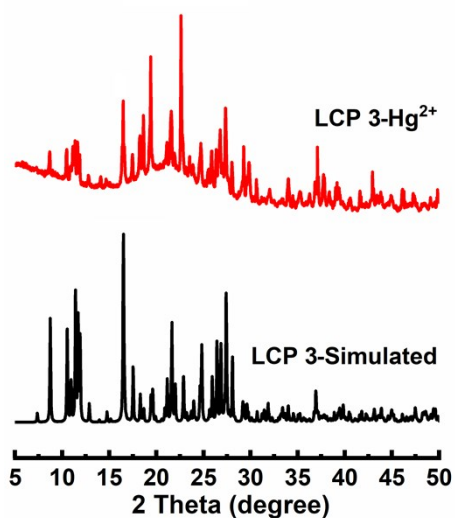


**Fig. S12.** The PXRD of LCP 3 after immersing in Hg(II) solution for 24h.

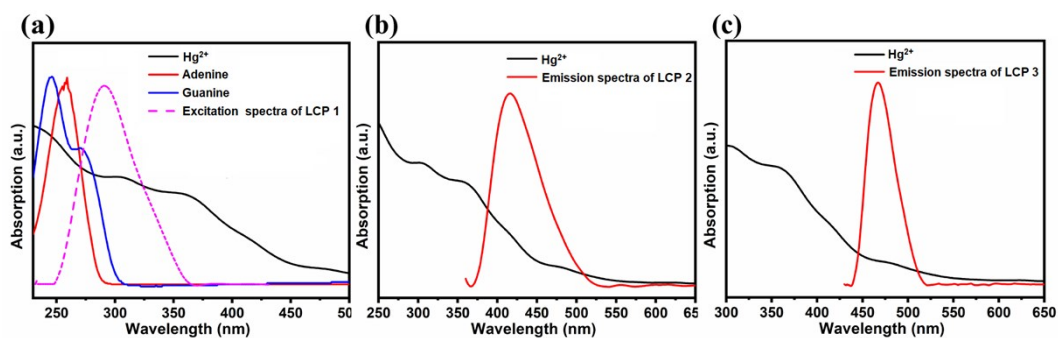


**Fig. S13.** UV-vis optical absorption spectra of analytes along with the excitation or emission spectra of LCPs 1–3.

## References

1. O. V. Dolomanov, L. J. Bourhis, R. J. Gildea, J. A. K., *J. Appl. Crystallogr.*, 2009, **42**, 339–341.
2. B. Chen, J. Ma, T. Yang, L. Chen, P. F. Gao, C. Z. Huang, *Biosens. Bioelectron.*, 2017, **98**, 36–40.
3. A. Meng, Q. Xu, K. Zhao, Z. Li, J. Liang, Q. Li, *Sens. Actuators B Chem.*, 2018, **255**, 657–665.
4. R. Duan, C. Li, S. Liu, *Spectrochimica Acta Part A: Molecular and Biomolecular Spectroscopy*, 2016, **152**, 272-277.
5. S. N. Tayade, A. K. Tawade, P. Talele, *Methods Appl. Fluoresc.*, 2019, **7**, 045002.
6. J. Li, J. Jiang, H. Feng, *RSC adv*, 2016, **6**, 31565-31573.
7. S. Pang, Y. Zhang, C. Wu, *Sens. Actuators B Chem.*, 2016, **222**, 857-863.
8. L. Li, Y. Lu, Y. Ding, *Can. J. Chem.*, 2012, **90**, 173-179.
9. Y. Cui, J. Yu, S. Feng, *Talanta*, 2014, **130**, 536-541.
10. S. N. Tayade, A. K. Tawade, P. Talele, *Methods Appl. Fluoresc.*, 2019, **7**, 045002.